Electronic Supplementary Material (ESI) for Journal of Materials Chemistry A.

Supporting Information

Enhancing the interfacial stability between argyrodite sulfide-based solid electrolytes and lithium electrodes through CO_2 adsorption

Shi-Kai Jiang[a], Sheng-Chiang Yang[a], Wei-Hsiang Huang[b], Hung-Yi Sung[a], Ruo-Yun Lin[a], Jhao-Nan Li[a], Bo-Yang Tsai[a], Tripti Agnihotri[a], Yosef Nikodimos[a], Chia-Hsin Wang[c], Shawn D. Lin[a], Chun-Chieh Wang[c], She-Huang Wu[b,*], Wei-Nien Su[b,*], Bing Joe Hwang[a,c,d,*]

a. NanoElectrochemistry Laboratory, Department of Chemical Engineering, National Taiwan University of Science and Technology, Taipei, 10607, Taiwan

b. NanoElectrochemistry Laboratory, Graduate Institute of Applied Science and Technology, National Taiwan University of Science and Technology, Taipei, 10607, Taiwan

c. Sustainable Energy Development Center, National Taiwan University of Science and Technology, Taipei, 10607, Taiwan

d. National Synchrotron Radiation Research Center, Hsin-Chu, 30076, Taiwan

Shi-Kai Jiang & Sheng-Chiang Yang contributed equally to this work

*Corresponding authors: bjh@mail.ntust.edu.tw (B. J. Hwang), wsu@mail.ntust.edu.tw (W.-N. Su) and wush88@gmail.com (S.-H. Wu)

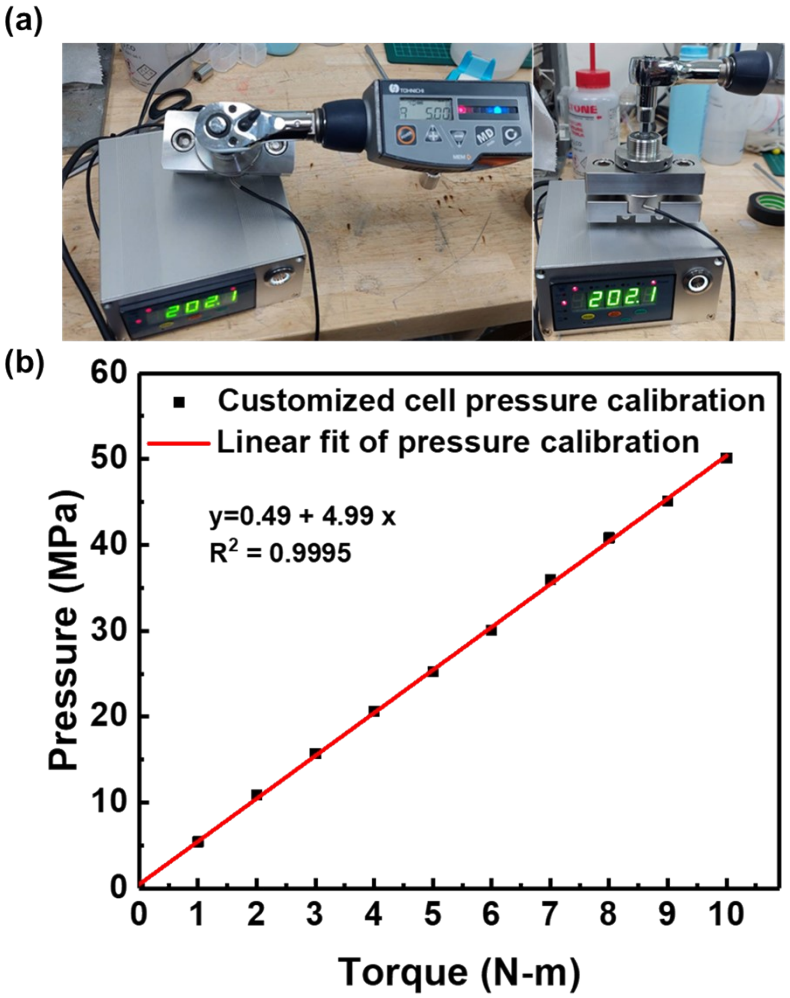

Fig. S1 Calibration line of pressure on GiT cell (a) the calibration device and Torque Wrench under 5 N-m (b) the calibration line and fitting curve.

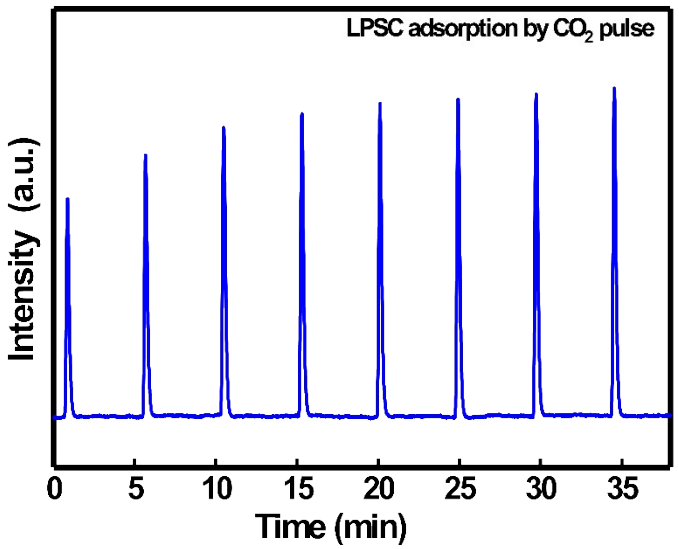

Fig. S2 The CO_2 pulse signal of LPSC adsorption. The 100 mg powder of LPSC was filled in between the quartz wool plugs inside a quartz tube and the sample was followed degassing at 30 c.c./min 5N He and heated to 400 °C with 10 °C/min, then cooled to 50 °C, and then CO_2 adsorption at 50 °C by 10% CO_2 + 90 % He with 30 c.c./min via the pulse injection (0.5 c.c. loop), until saturation

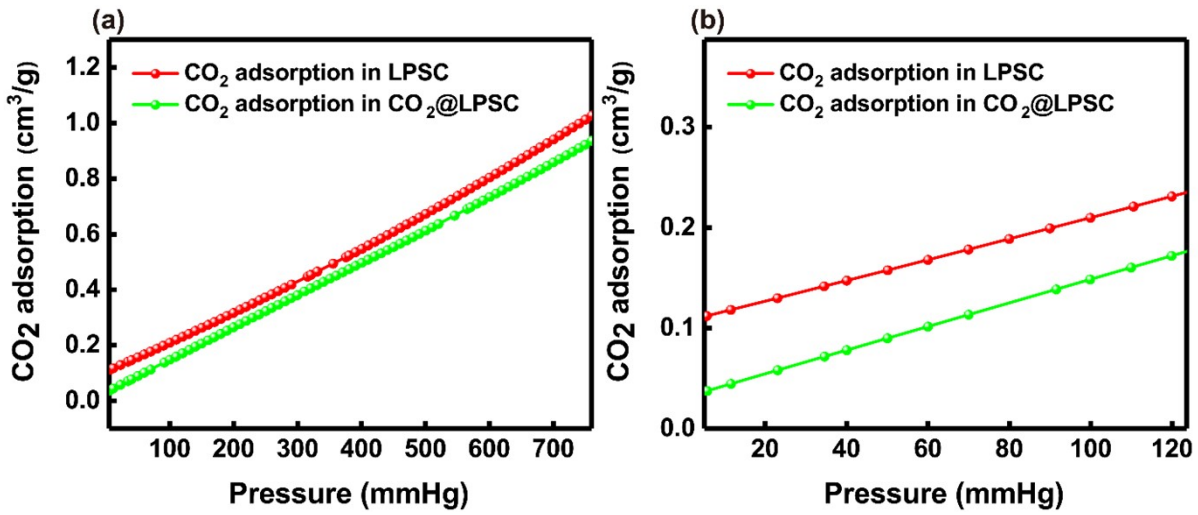

Fig. S3 The amount of CO_2 chemisorption from the BET measurement: (a) pristine LPSC and CO_2@LPSC, (b) magnification in the low-pressure region of (a).

***Holder of In-situ* DRIFTS**

From the TPD result, there is chemical adsorption between CO_2 and LPSC, In-situ DRIFTS analysis was built to understand the S-C bonding behavior. Because the LPSC has been unstable in the air, the LPSC sample will be sealed into the NICOLETTM iS50 holder and set the 2 pipelines for gas in (10% CO_2 + 90% He and Ar) and 1 pipeline for gas out in the system as shown in **Fig. S4.**

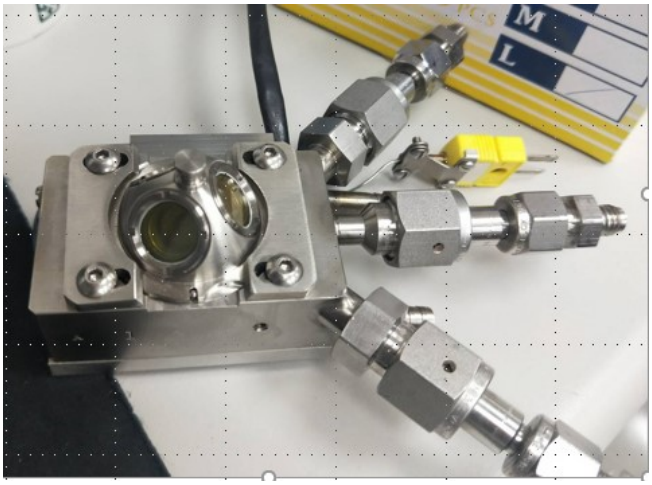

Fig. S4 The NICOLET™ iS50 *in situ* DRIFT holder, there are three channels for CO_2 gas in, Ar gas in and gas out. The 0.2 g LPSC powder was filled in the holder under Ar-filled glove box.

The thermal stability of LPSC material

To make sure the LPSC will not be damaged during the high temperature (400℃) desorption process under in-situ DRIFT measurement. The ex-situ XRD has been performed with the different temperature heat treatment LPSC sample as shown in **Fig. S5.** It is indicated that there is no structure variation after heat treatment.

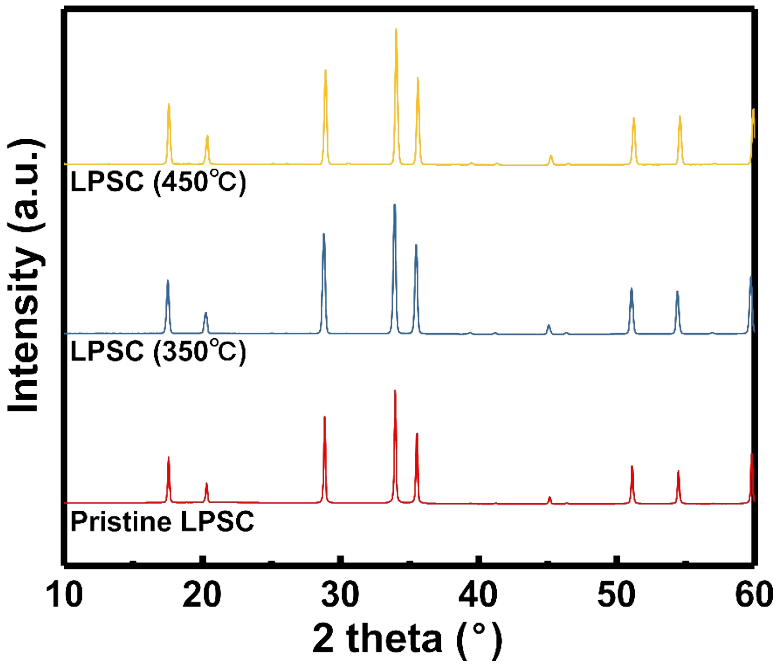

Fig. S5 XRD patterns of pristine LPSC and heat-treated LPSC.

Identify of the physiosorbed and chemisorbed

During the CO_2 purging process, there are physiosorbed and chemisorbed on the LPSC surface at the same time, to quick identification these two phenomena the LPSC would be purged the Ar gas in the final state. Comparing **Fig. 3**, shows the gas phase CO_2 at 2307 cm^{-1} and overtone signal of gas phase CO_2 and S-CO_2 at 3500-4000 cm^{-1} have been purged out.

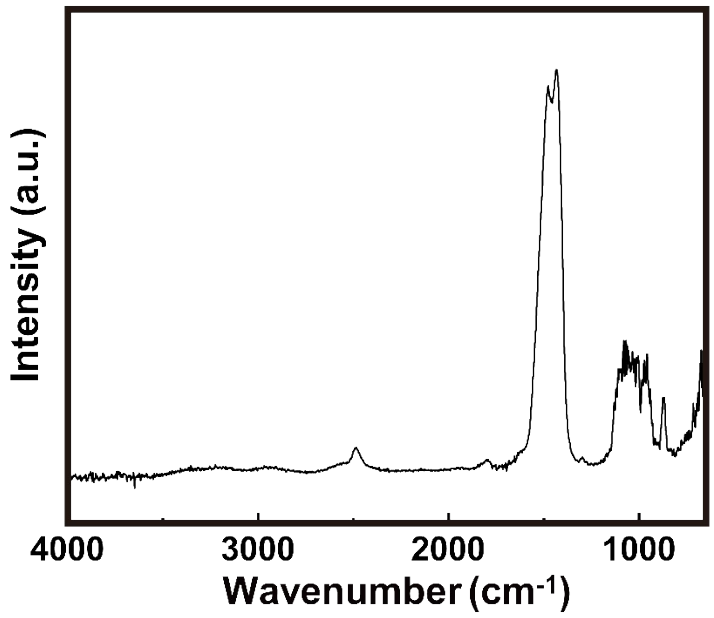

Fig. S6 FT-IR spectrum of Ar purged LPSC after CO_2 adsorption for 40 minutes

The S-CO_2 bonding verify via C-XPS

To prove the type of S-CO_2 bonding exists, the C-XPS was used to analyze the bonding form. However, due to the LPSC's high reactivity with the Cu tape to form CuS, thus, here using the carbon tape to adhesion the CO_2@LPSC powder. There is found a new peak at 289.6 eV which can be assigned to S-CO_2 in **Fig. S7**.

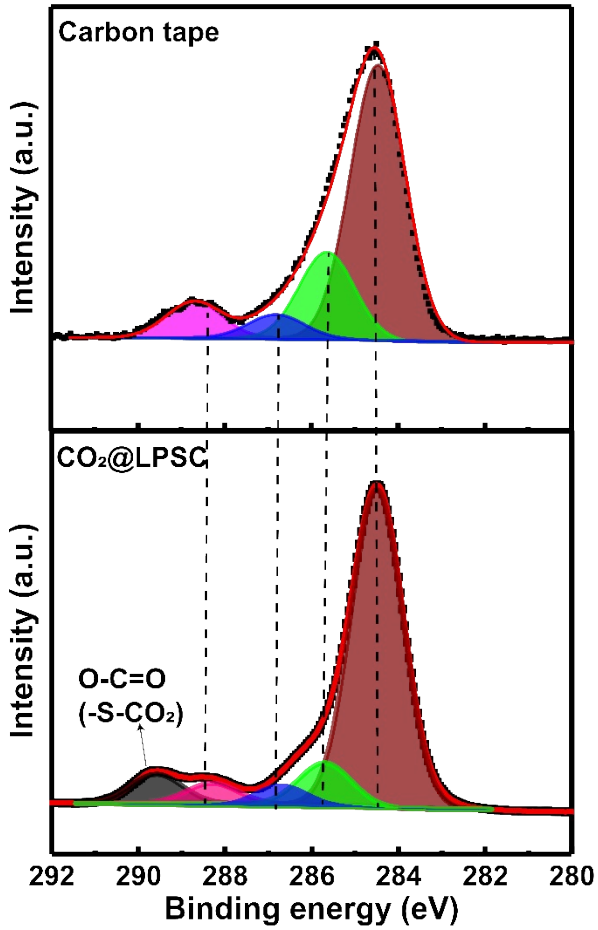

Fig. S7 XPS C $_{1s}$ spectra of carbon tape and CO_2@LPSC

The LPSC structure stability after S-CO_2 bonding forming.

To understand whether the S-CO_2 bonding is any side effects on LPSC structure or not, the ex-situ transmission XRD was performed, see **Fig. S8**. There is no structure change after S-CO_2 bonding forming.

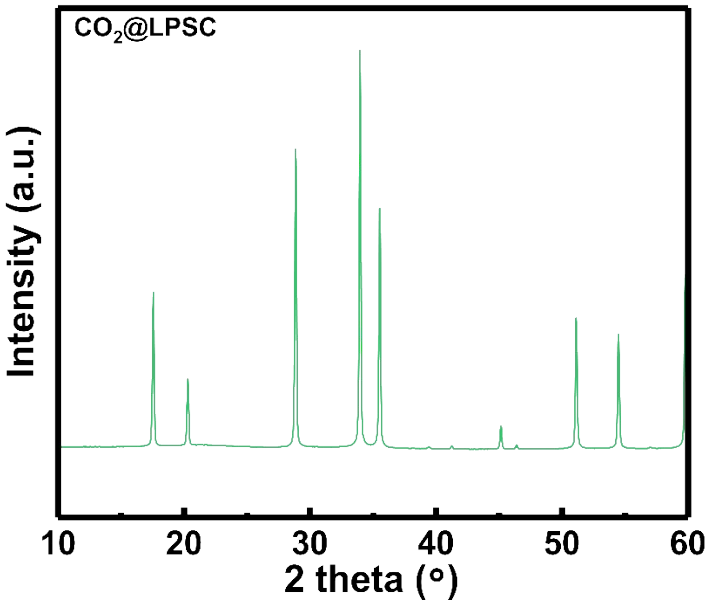

Fig. S8 XRD pattern of CO_2@LPSC

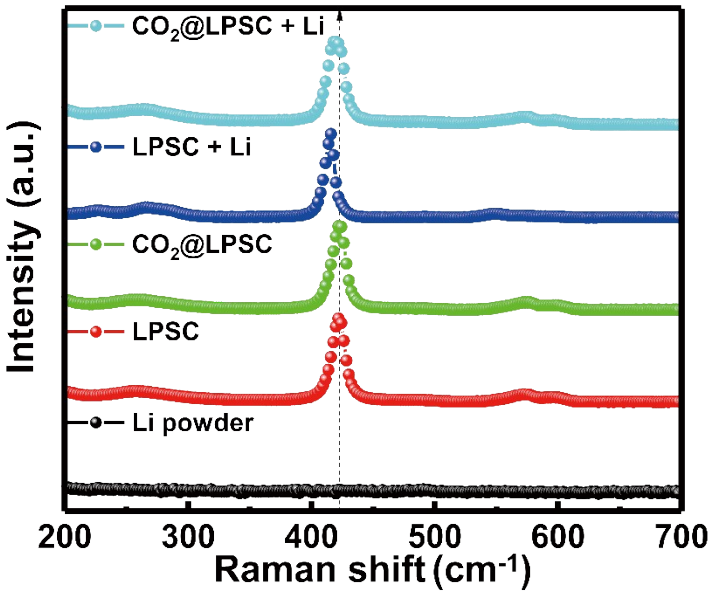

Fig. S9 The Raman spectra results of Li powder, LPSC, CO_2@LPSC, LPSC mixed with Li powder, and CO_2@LPSC mixed with Li powder.

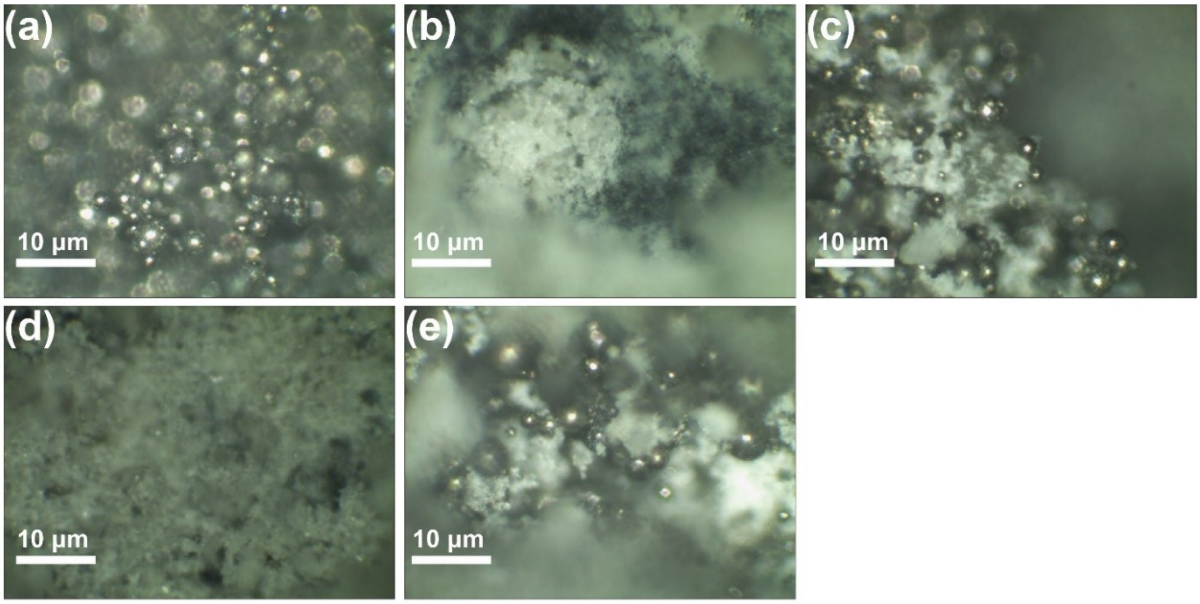

Fig. S10 The optical microscopy results of (a) Li powder, (b) LPSC (c) LPSC mix with Li, (d) CO_2@LPSC, and (e) CO_2@LPSC mixed with Li powder

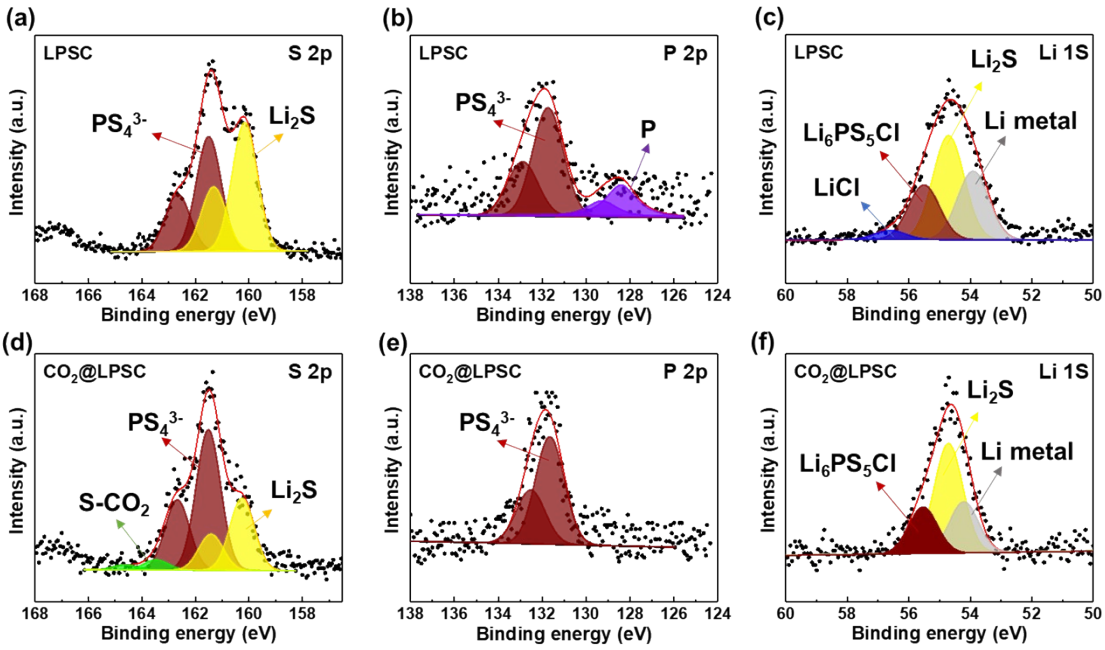

Fig. S11 XPS spectra of the decomposed products at Li/LPSC and Li/CO_2@LPSC. (a) XPS S 2p spectrum of LPSC (b) XPS P 2p spectrum of LPSC (c) XPS Li 1s spectrum of LPSC (d) XPS S 2p spectrum of CO_2@LPSC (e) XPS P 2p spectrum of CO_2@LPSC (f) XPS Li 1s spectrum of CO_2@LPSC

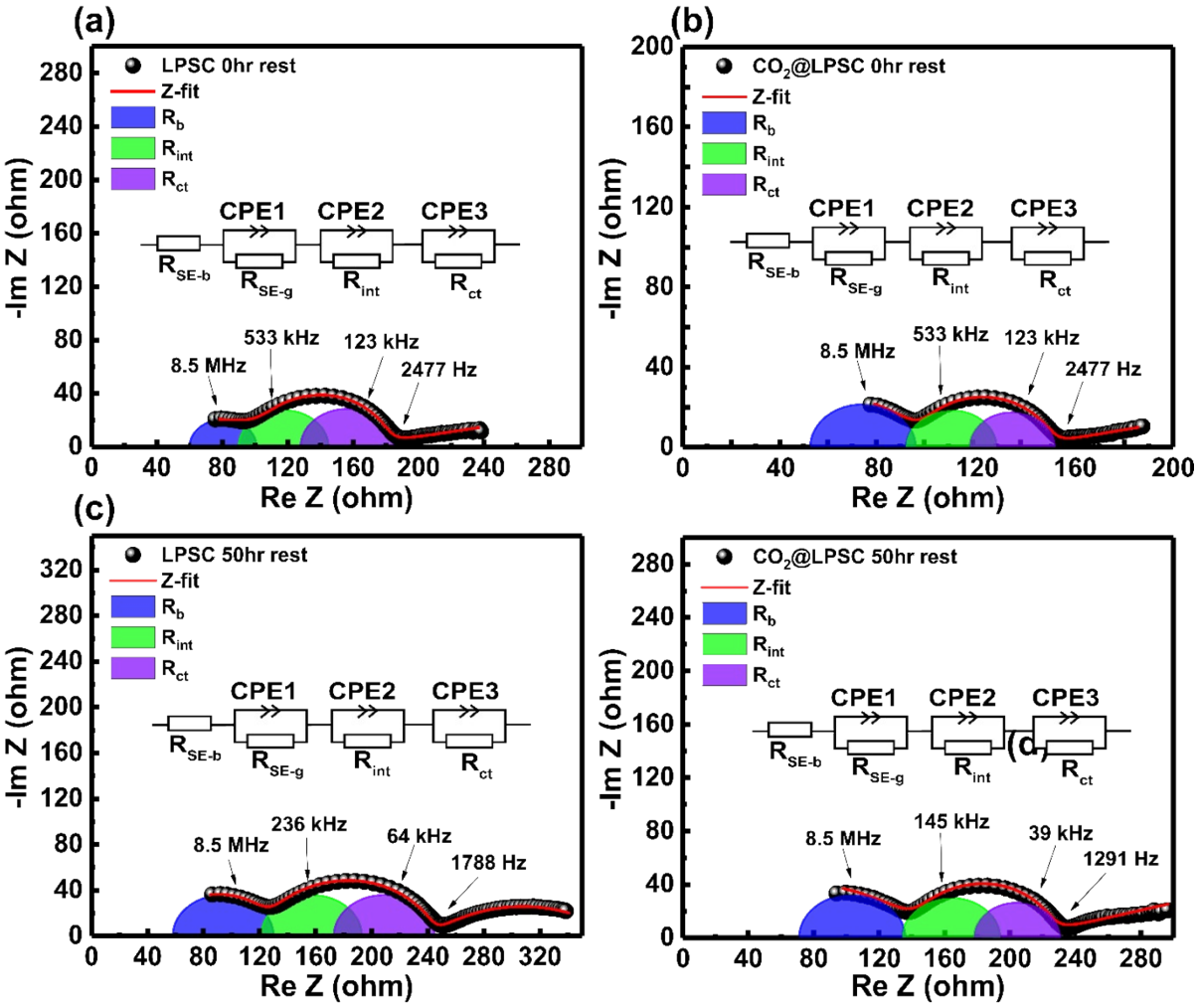

Fig. S12 The time evolution impedance fitting of: (a) Li|LPSC|Li at 0-hour, (b) Li|CO_2@LPSC|Li at 0-hour, (c) Li|LPSC|Li at 50 hours, and (d) Li|CO_2@LPSC|Li at 50 hours.

Table S1 The EIS fitting parameters of Li|LPSC|Li

Li|LPSC|Li			
Rest time (hr)	**R_{SE-b} +R_{SE-g} (ohm)**	**R_{int} (ohm)**	**R_{ct} (ohm)**
1	**41**	**55**	**57**
2	**66**	**67**	**67**
5	**69**	**70**	**59**
10	**66**	**68**	**59**
15	**72**	**71**	**62**
20	**72**	**72**	**62**
25	**73**	**72**	**65**
30	**72**	**73**	**64**
35	**71**	**72**	**64**
40	**72**	**75**	**68**
45	**73**	**75**	**70**
50	**72**	**72**	**72**

Table S2 The EIS fitting parameters of Li|CO_2@LPSC|Li

Li|CO_2@LPSC|Li			
Rest time (hr)	**R_{SE-b} +R_{SE-g} (ohm)**	**R_{int} (ohm)**	**R_{ct} (ohm)**
1	**43**	**37**	**35**
2	**65**	**50**	**38**
5	**68**	**51**	**42**
10	**68**	**53**	**42**
15	**65**	**54**	**42**
20	**68**	**55**	**47**
25	**61**	**56**	**47**
30	**64**	**57**	**47**
35	**60**	**58**	**47**
40	**62**	**60**	**48**
45	**62**	**60**	**48**
50	**61**	**62**	**50**

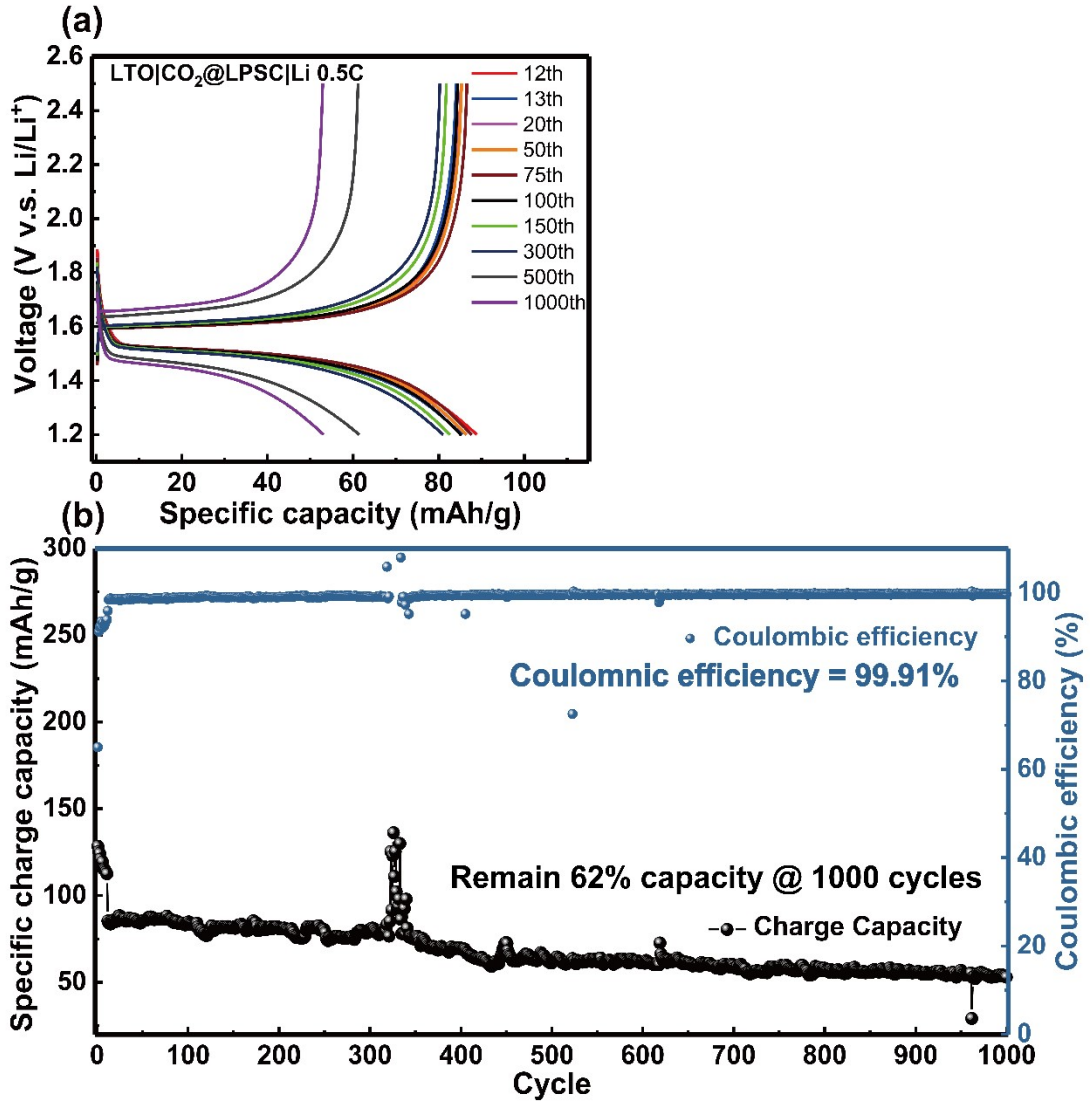

Fig. S13 The Li|CO_2@LPSC|LTO half-cell measurement (a) charge-discharge profile under 0.5C in the previous 12 to 1000 cycles, (b) the specific charge capacity and coulombic efficiency analysis in 1000 cycles.

Table S3 Summary of the Li|SSE|LTO long-term coulombic efficiency and charge capacity

System	1st CE (%)	Q (mAh/g) (1st)	Avg. CE (%) (1st~150th)	Q (mAh/g) (12th)	Q (mAh/g) (150th)	High rate Retention (%) (12th - 150th)
Li|LPSC|LTO	57.5	112	97.6	70.5	60.6	85.8
Li|CO_2@LPSC|LTO	65	128	98.1	85.2	81.7	96

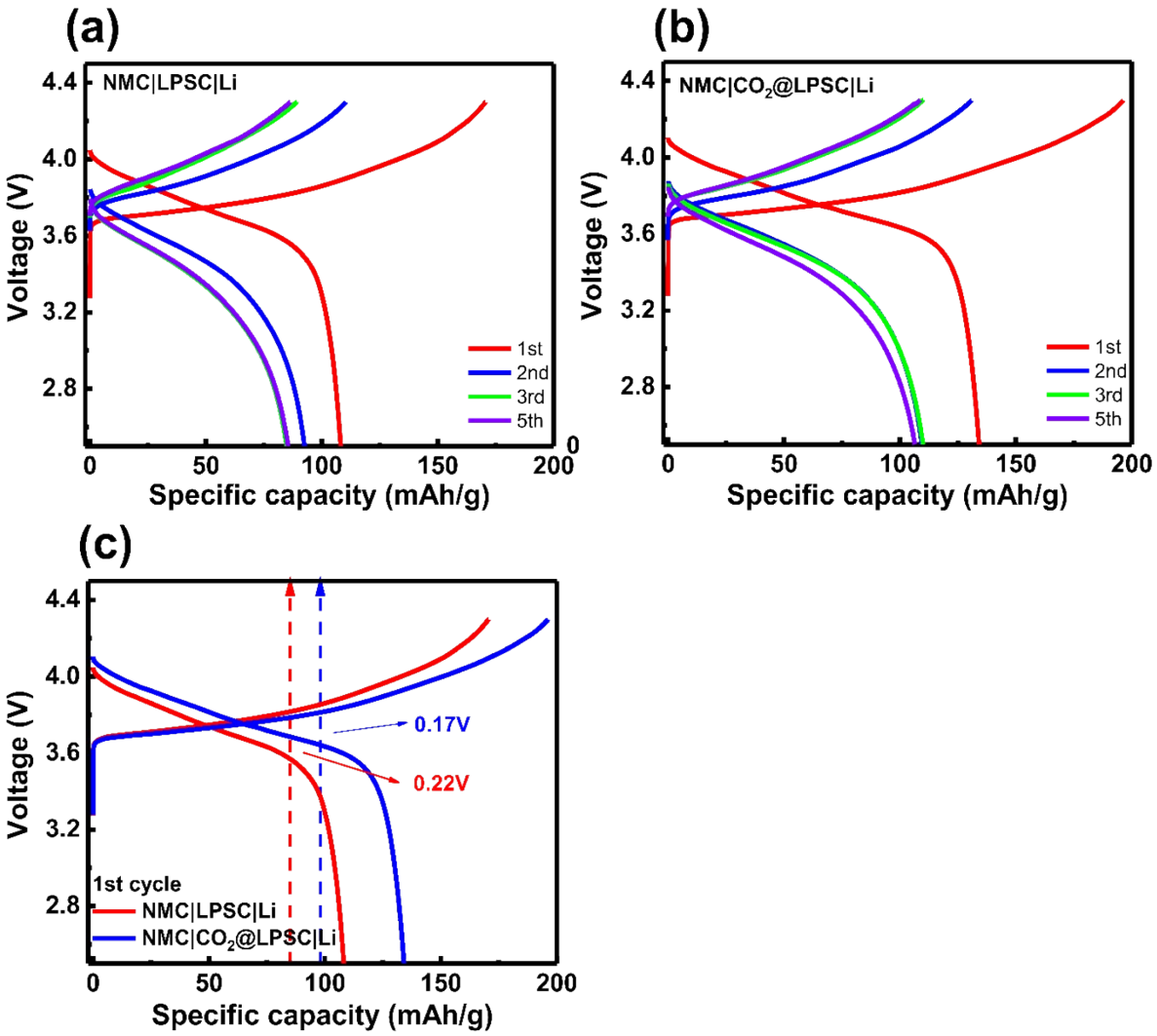

Fig. S14 The charge-discharge curves of pristine and CO_2 @LPSC in LNO@NMC|Li configuration. The LNO@NMC811|SSE|Li was assembled with 10 mm Li and the 10 – 15 mg LNO@NMC811 pellet preparation was done using cold-press with 300 MPa for the 30 s. The performance was cycled under 0.05 C for the first cycle, and after the second cycle the charge and discharge rate were used 0.05 C and 0.2 C, respectively.

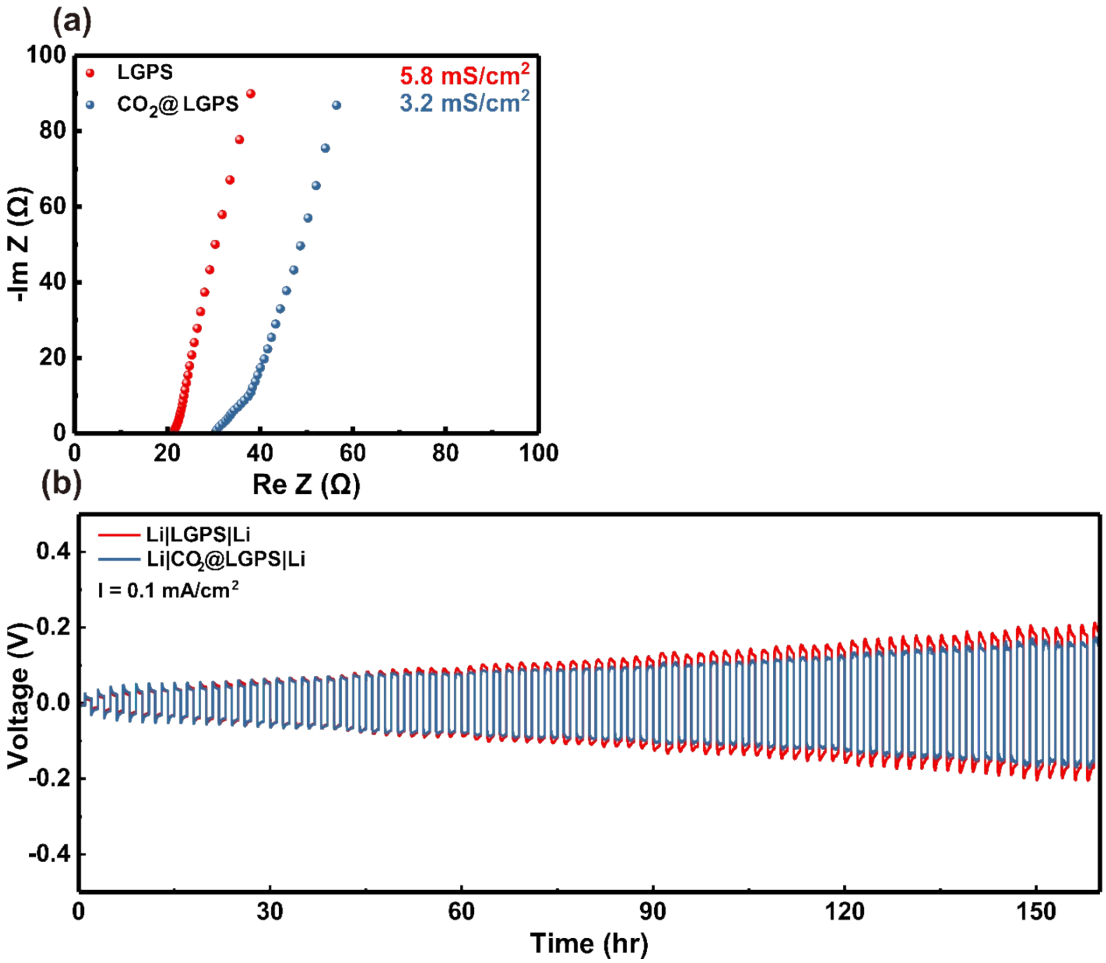

Fig. S15 The pristine and CO_2@LGPS of: (a) ionic conductivity measurement, and (b) Li|Li symmetry cell performance. The ionic conductivity measurement was performed in stainless steel blocking electrode from 10 M Hz to 1 Hz. The Li|Li symmetry-cell was performed under 0.1 mA/cm^2 and 1.2 N-m torque with a diameter of 10 mm 100 mg SSE pellet. All the pellet was prepared by 300 M Pa cold-pressed.